Supporting Information for

Unusual thermal boundary resistance in halide perovskites: A way to tune ultralow thermal conductivity for thermoelectrics

Tianjun Liu,[†,#] Sheng-Ying Yue,[‡,ǁ,#] Sinclair Ratnasingham,[§] Thibault Degousée,[†] Pritesh Varsini,[†] Joe Briscoe,[†] Martyn A. McLachlan,[§] Ming Hu[‡,⊥] and Oliver Fenwick[†,*]

[†]School of Engineering and Materials Science, Organic Thermoelectrics Laboratory, Materials Research Institute, Queen Mary University of London, Mile End Road, London E1 4NS, UK. *Email: o.fenwick@qmul.ac.uk

[‡]Institute of Mineral Engineering, Division of Materials Science and Engineering, Faculty of Georesources and Materials Engineering, Aachen Institute for Advanced Study in Computational Engineering Science (AICES), RWTH Aachen University, 52062 Aachen, Germany.

[ǁ]Department of Mechanical Engineering, University of California, Santa Barbara, CA, 93106, USA.

[§]Department of Materials and Centre for Plastic Electronics, Imperial College London, London SW7 2AZ, UK.

[⊥]Department of Mechanical Engineering, University of South Carolina, Columbia, SC 29208, USA

[#] T. Liu and S.-Y. Yue made equal contributions to this work.

Density functional theory (DFT) method.

The phonon modes of $MAPbI_3$ were calculated via the finite displacement difference method implemented in the PHONOPY package[1]. We calculated the phonon dispersion based on density functional theory using VASP code package. The Perdew-Burke-Ernzerhof parametrization of the generalized gradient approximation (GGA)[2] was applied for the exchange-correlated functional, and the projector-augmented wave (PAW)[3, 4] method was used to model the core electrons (for Pb the 5d orbitals are included). The energy-cutoff of plane wave was set as 700 eV. For the parameter of the partial occupancies we adopted the Gaussian smearing and the width of the smearing was 0.01 eV. The van der Waals (vdW) interactions were also considered here as non-bonded terms[5]. When we calculated the low-frequency phonon dispersion of the orthorhombic and tetragonal phases, we considered the whole MA molecule as a rigid object, meaning that we froze its inner freedoms. The unit cell of the orthorhombic and tetragonal phases contains 48 atoms. We adopted 2 × 2 × 2 supercell for the both phases and used 6 × 6 × 6 Monkhorst-Pack grids as k-point sampling. The phonon group velocities (v_g) can be obtained by $v_g = \frac{d\omega}{dk}$, where ω is the phonon frequency and k is the momentum vector of phonons in k space. Simultaneously, we obtain the partial density of states (PDOS) and the free energy, the inner energy, the entropy and the phonon heat capacity with PHONOPY package[1].

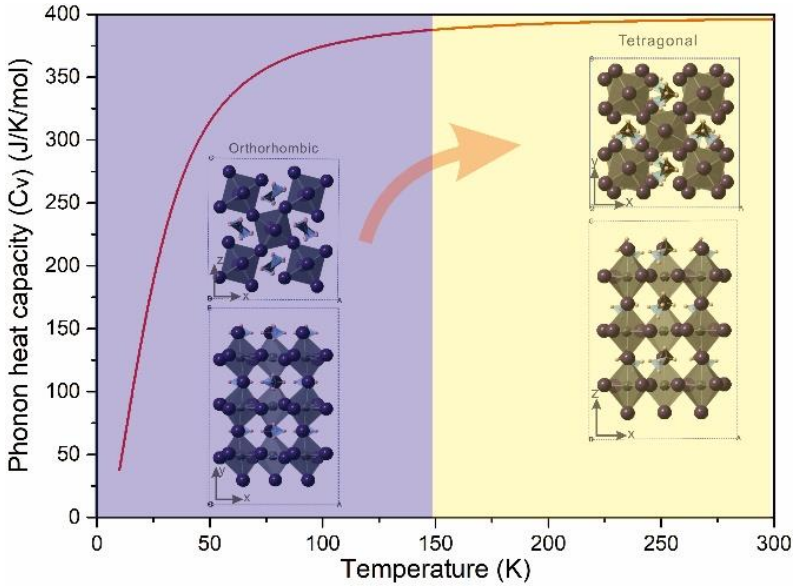

Figure S1. Heat capacity of phonons changing with temperature of orthorhombic and tetragonal phases of $MAPbI_3$.

Thickness dependence of thermal conductivity of $MAPbI_3$ thin films deposited by AACVD method.

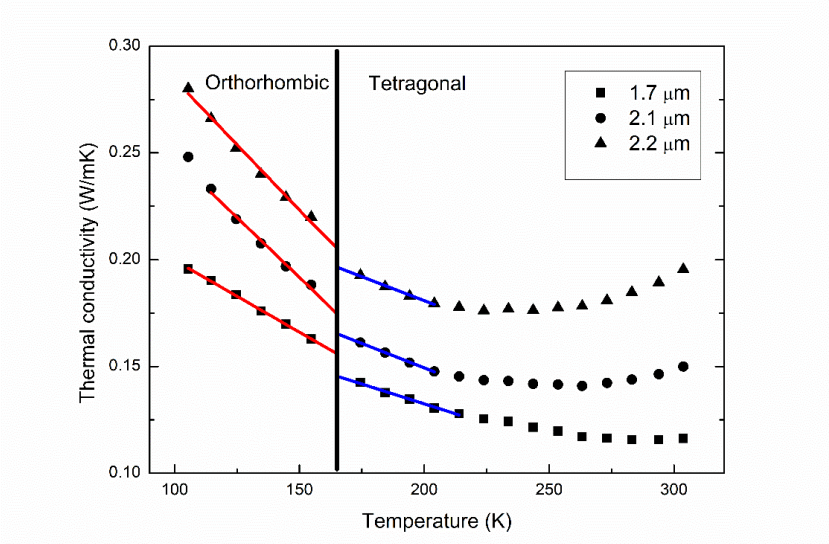

Figure S2. Temperature-dependent thermal conductivity values from 100 K to 300 K of perovskite films with CVD method. The values of 1.7μm, 2.1μm and 2.2μm films corresponded to black, red and blue dots, respectively.

The Kapitza resistance fitting.

The Kapitza resistance expresses the thermal boundary resistance present either at the interfaces of two materials or grains of the same material with the macroscopic effective medium approach (EMA). The model describes the observed crystallite-size (d) dependent κ of polycrystalline materials and, most importantly, offers a simple and practical method to determine the Kapitza resistance.

$$\kappa(T,d) = \frac{\kappa_i}{1 + \frac{R_k \kappa_i}{d}} \quad equation\ 1$$

$$\frac{1}{\kappa} = \frac{1}{\kappa_i} + \frac{R_k}{d} \quad equation\ 2$$

The crystallite-size (d) is estimated by Scherrer equation, d=Kλ/Bcosθ , B is line broadening at full width at half maximum (FWHM) after substracting instrumental line broadening, K is a dimensionless shape factor (here is 0.9), λ is X-ray wavelength (1.54 Å). By fitting the experimental data of $1/\kappa$ against $1/d$ at each temperature, assuming a liner approximation for all the samples, we can get two parameters of the Kapitza resistance R_k and the intrinsic thermal conductivity κ_i from equation 2. The errors on these values reported in the main text come from the fitting errors of the $1/\kappa$ against $1/d$ plot.

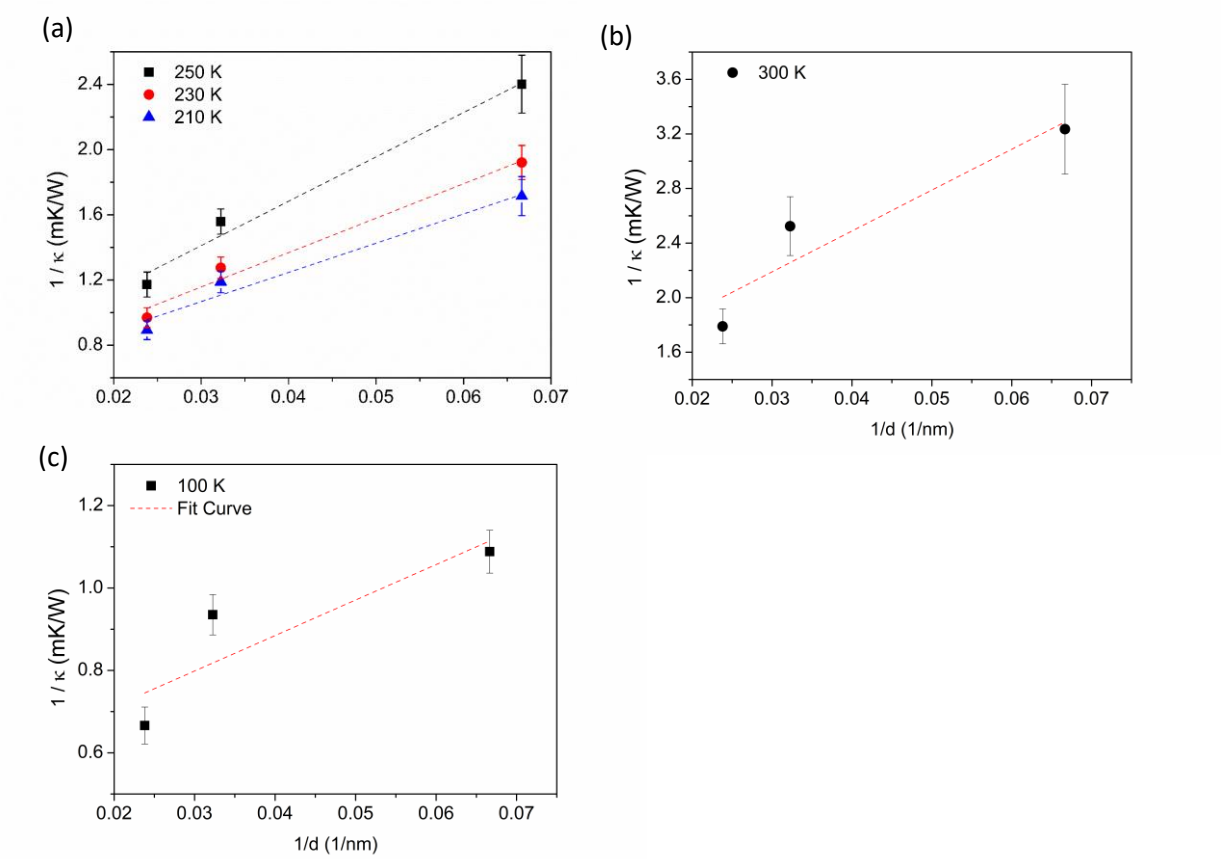

Figure S3. (a) $1/\kappa$ *versus* 1/d plots for different grain sizes at 210 K, 230 K and 250 K. (b) 300 K and (c) 100 K. The dots are experimental data, while the lines are calculated according to the fit of equation 2 to the experimental data. Herein, the values of R_k were obtained from the slope of the curves, the values of κ_i were got from the inverse of intercept.

Thermal conductivity measurement.

An alternating current $I(t) = I_0 \times \cos(\omega t)$ is used to heat the stripe. Joule heating occurs at frequency 2ω due to the heating power, $I_\omega^2 = I_0^2 R(1 + \cos(2\omega t))/2$. As a result, the temperature oscillates at 2ω, and the temperature dependent electrical resistance also has a component at 2ω ($R_{2\omega}$). The temperature change of the heating stripe is measured with a lock-in amplifier which can extract the third harmonic of the voltage drop across the heating stripe ($V_{3\omega} = I_\omega R_{2\omega}$). The third-harmonic voltage captures the second-harmonic temperature rise ($\Delta T_{2\omega}$) in the heater, which is a function of the thermal properties of the underlying materials. Considering in-plane thermal conductivity, by solving the two dimensional partial differential heat equation across the membrane with the given boundary conditions, the general expression for the amplitude of the 3ω oscillation $V_{3\omega}$ is expressed as[6]:

$$|V_{3\omega}| = \frac{\beta R^2 I_0^3}{4\left(\frac{2\kappa t l}{w}\right)\sqrt{1 + \omega^2\left(4\tau^2 + \frac{w^4}{24D^2} + \frac{\tau w^2}{3D}\right)}} \quad equation\ 3$$

where β is the temperature coefficient of resistance, t is the total thickness of sample plus 100nm of Si_3N_4 membrane and 33 nm of Al_2O_3, l is the length of the heater, w is the width of the membrane, τ is the thermal relaxation time, $D = \kappa/\rho c$, where ρ is the mass density and c is the specific heat capacity. When using low frequencies, the measurement can be performed at quasi-steady state

conditions, where the ω becomes negligible and $V_{3\omega}$ becomes constant. Equation 3 can be written as:

$$V_{3\omega} = \frac{\beta R^2 I_0^3}{4(\frac{2\kappa t l}{w})} \; equation\ 4$$

To get the thermal conductivity of the sample, the contribution of membrane thermal conductance should be removed. The sample thermal conductivity is given by

$$\kappa_{sample} = \frac{\kappa t - \kappa_m t_m}{t_s} \; equation\ 5$$

Where κ_m is the membrane thermal conductivity, t_m is the membrane thickness, t_s is the sample thickness.

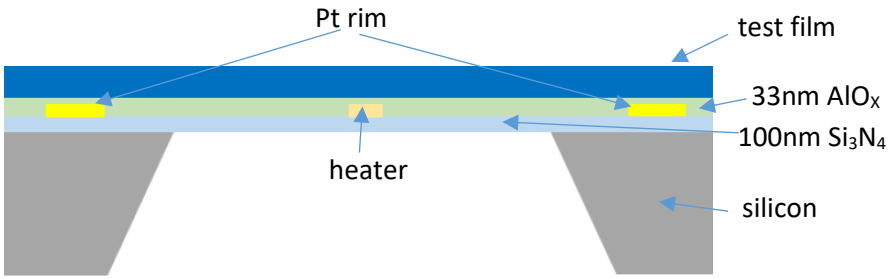

Figure S4. Schematic structure of ZT chip (Linseis Messgeräte GmbH). The 100 nm Si_3N_4 membrane is framed by a Pt rim to act as a heat sink on the cold side. The heating stripe is positioned along the centre of the membrane for the heating and monitoring temperature. The heating stripe is electrically isolated from the film under test by a 33 nm Al_2O_3 passivation layer.

References

1. Togo, A.; Tanaka, I., First Principles Phonon Calculations in Materials Science. *Scripta. Mater.* **2015,** *108*, 1-5.
2. Perdew, J. P.; Burke, K.; Ernzerhof, M., Generalized Gradient Approximation Made Simple. *Phys. Rev. Lett.* **1996,** *77* (18), 3865-3868.
3. Blochl, P. E., Projector Augmented-Wave Method. *Phys. Rev. B* **1994,** *50* (24), 17953-17979.
4. Kresse, G.; Joubert, D., From Ultrasoft Pseudopotentials to The Projector Augmented-Wave Method. *Phys. Rev. B* **1999,** *59* (3), 1758-1775.
5. Tkatchenko, A.; Scheffler, M., Accurate Molecular Van Der Waals Interactions from Ground-State Electron Density and Free-Atom Reference Data. *Phys. Rev. Lett.* **2009,** *102* (7).
6. Linseis, V.; Volklein, F.; Reith, H.; Woias, P.; Nielsch, K., Platform for In-Plane ZT Measurement and Hall Coefficient Determination of Thin Films in A Temperature Range from 120 K up to 450 K. *J. Mater. Res.* **2016,** *31* (20), 3196-3204.